



Synthesis and enzymatic cleavage of dual-ligand quantum dots

Sarah L. Sewell^a, Todd D. Giorgio^{a,b,*}

^a Department of Biomedical Engineering, Vanderbilt University, Nashville, TN, USA

^b Department of Chemical and Biomolecular Engineering, Vanderbilt University, Nashville, TN, USA

ARTICLE INFO

Article history:

Received 11 July 2008

Received in revised form 20 October 2008

Accepted 15 November 2008

Available online 27 November 2008

Keywords:

Quantum dot

Dual-ligand

MMP-7

Targeted therapy

Nanotechnology

Tissue specific targeting

ABSTRACT

Site directed therapy promises to minimize treatment-limiting systemic effects associated with cytotoxic agents that have no specificity for pathologic tissues. One general strategy is to target cell surface receptors uniquely presented on particular tissues. Highly specific *in vivo* targeting of an emerging neoplasm through a single molecular recognition mechanism has not generally been successful. Nonspecific binding and specific binding to non-target cells compromise the therapeutic index of small molecule, ubiquitous cancer targeting ligands. In this work, we have designed and fabricated a nanoparticle (NP) construct that could potentially overcome the current limitations of targeted *in vivo* delivery. Quantum dots (QDs) were functionalized with a poly(ethylene glycol) (PEG) modified to enable specific cleavage by matrix metalloprotease-7 (MMP-7). The QDs were further functionalized with folic acid, a ligand for a cell surface receptor that is overexpressed in many tumors, but also expressed in some normal tissues. The nanomolecular construct is designed so that the PEG initially conceals the folate ligand and construct binding to cells is inhibited. MMP-7 activated peptide cleavage and subsequent unmasking of the folate ligand occurs only near tumor tissue, resulting in a proximity activated (PA) targeting system. QDs functionalized with both the MMP-7 cleavable substrate and folic acid were successfully synthesized and characterized. The proteolytic capability of the dual ligand QD construct was quantitatively assessed by fluorometric analysis and compared to a QD construct functionalized with only the PA ligand. The dual ligand PA nanoparticles studied here exhibit significant susceptibility to cleavage by MMP-7 at physiologically relevant conditions. The capacity to autonomously convert a biopassivated nanostructure to a tissue-specific targeted delivery agent *in vivo* represents a paradigm change for site-directed therapies.

© 2008 Elsevier B.V. All rights reserved.

1. Introduction

Many current cancer treatments produce nonspecific injury to cancer and normal tissues, leading to systemic toxicity. Ideally, targeted therapies would preferentially deliver anticancer agents to tumor tissues and spare normal tissues. First generation targeted therapies used site-specific ligands directed to the surface of cancer cells [1–4]. Unfortunately, nonspecific binding and specific binding to non-tumor cells diminished the effectiveness of early targeted drug delivery approaches, especially for small molecular weight ligands [5,6]. Second generation targeted therapies have evolved that employ proteolytically cleavable substrates to reduce nonspecific interactions [7–12]. These substrates have been utilized in the design of imaging agents [7–10,12] and several prodrugs [13–15].

One such substrate, the peptide sequence RPLALWRS, is cleavable by MMP-7 (also known as matrilysin). MMP-7 is a zinc-dependent metalloprotease that is involved in the degradation of extracellular matrix and tumor progression. MMP-7 is also active in the progression of breast and colon cancer [12,16,17] and has been used as a diagnostic

marker for ovarian, pancreatic, esophageal and colon cancers [18–22]. Furthermore, the enzyme has been shown to be secreted at the earliest stages of cancer development by precancerous lesions [23,24]. Previously, McIntyre et al. have shown that MMP-7 cleaves RPLALWRS that has been functionalized on a PAMAM dendrimer *in vivo* [12].

Proteolytically cleavable peptides have also been conjugated to nanoparticles for use in imaging applications [25]. Nanoparticles are particularly advantageous for targeted therapies due to the large surface to volume ratio compared to molecular constructs, which allows many reactive ligands to be conjugated to the surface. A stable, covalent conjugation of an MMP-7 cleavable construct to a quantum dot (QD) has been reported by Smith et al. [25]. The MMP-7 cleavable construct consists of the RPLALWRS peptide sequence flanked by two polyethylene (PEG) groups. The PEG groups reduce the nonspecific binding of the particle [26,27]. When the construct is in the proximity of MMP-7, the peptide is cleaved, hence the construct is “proximity activated” (PA) [25].

In this work, we have extended the effort of Smith et al. [25] to create a dual-ligand QD functionalized with both the PA construct and folic acid, a tissue specific small molecule [28,29]. Folic acid receptors are over-expressed in many human cancers including breast, ovarian, brain, kidney, and lung [30]. Furthermore, a study by Hartman et al. concluded that breast cancer patients with primary tumors that express folic acid

* Corresponding author. Vanderbilt University, Box 351620, Station B, Nashville, TN 37235, USA. Tel.: +1 615 322 3756; fax: +1 615 343 7919.

E-mail address: todd.d.giorgio@vanderbilt.edu (T.D. Giorgio).

receptors were more aggressive and correlated to disease recurrence and reduced patient survival [31]. Folic acid receptors, however, are expressed by normal tissues such as the kidney, intestine and lung, compromising specificity as a tumor-targeting agent [30,32–35]. In the multifunctional nanoparticle designed here, the PA construct conceals the folic acid ligand until the particle is in the proximity of the tumor (Fig. 1). The folic acid is revealed upon PA cleavage, enabling highly specific tumor tissue targeting in the proximity of cleavage. A novel chemistry application has been used to synthesize a multifunctional nanoparticle (FA-QD-PA) with two different ligands, folic acid and the PA construct. Additionally, the cleavage of FA-QD-PA has been analyzed using exogenous MMP-7 *in vitro*.

Autonomous unmasking of a targeting ligand only in the proximity of an emerging neoplasm is the critical feature of the imaging nanoconstruct described here. The construct would be administered as a PEGylated nanoparticle, projected to possess the prolonged cardiovascular half-life and limited nonspecific binding characteristic of this class of materials [26,27]. MMP-7, a protease secreted from neoplasm, cleaves a peptide that bridges the PEG and the nanoparticle core of the construct. As the PEG and peptide stub diffuse away from the construct, the targeting ligand is revealed, facilitating specific recognition of the imaging nanoparticle with the neoplastic cells in the proximity of the relatively high MMP-7 concentration. This approach requires colocalization of two different characteristics of neoplasm for specific recognition: MMP-7 secretion and folate receptor expression on the cell surface. The PEG 'barrier' offers a significant obstruction to the folate recognition that would otherwise occur on some non-target cells. The requirement for local MMP-7 to reveal the folate ligand ensures that the construct will only actively target in the proximity of a neoplasm.

2. Materials and methods

2.1. Materials

The PA construct, PEG₃₄₀₀-[Ahx]-RPLALWRS-[Ahx]-PEG₅₀₀₀-K(5-FAM)-NH₂, was purchased from AnaSpec Corporation (San Jose, CA). This structure consists of a cleavable 8-mer peptide substrate (RPLALWRS) flanked by PEG groups with a molecular (feed) weight of 3400 and 5000. The PA construct also contains aminohexanoic acid (Ahx) groups that function as spacer molecules as well as a fluorescent tag (5-carboxyfluorescein, 5-FAM) for cleavage detection. The N-terminus of the construct was a primary amine to facilitate further conjugation reactions. Ac-terminal amidation was performed during the synthesis to stabilize the substrate and prevent additional modification during subsequent chemical reactions. During the

amidation the c-terminus is converted to a secondary amine, which is unreactive in EDC coupling reactions [36]. Carboxylated 585 QDs were purchased from Invitrogen Corporation (Carlsbad, CA). Exogenous matrixin (MMP-7) was purchased from Calbiochem (San Diego, CA). All other reagents were purchased from Sigma Aldrich.

2.2. QD-PA conjugation

The PA construct was conjugated to carboxylated 585 QDs (CdSe with a ZnS coating) by an 1-ethyl-3(3-dimethyl aminopropyl) carbodiimide (EDC) reaction. N-hydroxy succinimide (NHS) was omitted during the conjugation, resulting in unfunctionalized carboxylic acid groups that can be used to conjugate FA to the QD-PA. The PA construct (80 μ L, 10 mg/mL feed weight of 0.80 mg) was added to 1.87 mL of 1 μ M QDs in 10 mM borate buffer at pH 7.4. To facilitate the coupling, 57 μ L of EDC was added and the reaction stirred for 2 h. Molecular weight cutoff filters (100 kDa) were used to remove unreacted PA from the final QD-PA construct. The QD-PA construct was washed three times with 10 mM borate buffer at pH 7.4 to ensure purity [25].

2.3. QD-PA cleavage by MMP-7

The ability of the QD-PA construct to function as a cleavable substrate was investigated using exogenous MMP-7. MMP-7 (20 μ L) was added to the QD-PA construct (100 μ L, 100 nM) to achieve a final concentration of 100 nM MMP-7 in 10 mM borate buffer fortified with 50 μ M ZnSO₄ at pH 7.4. The final volume of the reaction was 200 μ L and the final concentration of QD-PA was 50 nM. The reaction was incubated for 24 h at 37 °C. Cleaved peptide was removed from the reaction by filtration using a 100 kDa molecular weight cutoff filter. The QD-PA construct was washed three times with 10 mM borate buffer at pH 7.4. Control samples were prepared in the same fashion with MMP-7 omitted [25].

2.4. QD-FA conjugation

QDs were functionalized with folic acid via an EDC reaction. NHS (0.05 M in 10 mM borate buffer, pH 7.4) and EDC (0.05 M in 10 mM borate buffer, pH 7.4) were added to 100 μ L of 1 μ M carboxylated QDs. The reaction was stirred for 30 min at room temperature. The addition of EDC and NHS to the carboxylated QD forms a highly reactive carboxylate-NHS intermediate that will react with the amine of the folic acid. After 30 min, 100 μ L of 125 μ M folic acid in 10 mM borate buffer was added. The reaction stirred for 2 h at room temperature. The QD-FA conjugate was purified using 3.5 kDa molecular weight

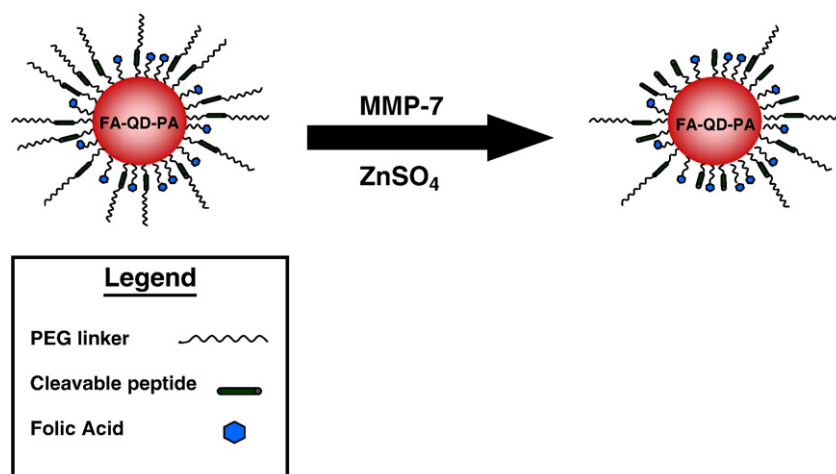


Fig. 1. Schematic of the cleavage of the FA-QD-PA nanoparticle by MMP-7. Upon the addition of MMP-7, the PA construct is cleaved revealing the FA.

dialysis kit for 24 h with 3 buffer exchanges. The conjugates were washed three times with 10 mM borate buffer at pH 7.4.

2.5. QD-PA conjugation with FA

An EDC/NHS coupling reaction was used to functionalize the pre-synthesized QD-PA construct with folic acid. EDC (0.05 M in 10 mM borate buffer, 25 μ L) and 25 μ L of 0.05 M NHS in 10 mM borate buffer was added to 1 mL of 0.15 μ M QD-PA conjugate. The reaction was stirred for 30 min at room temperature followed by addition of 500 μ L of 125 μ M (feed weight 27.85 μ g) folic acid in 10 mM borate buffer. The reaction was stirred for 2 h and was purified using 3.5 kDa molecular weight dialysis kit for 24 h with 3 buffer exchanges.

2.6. FA-QD-PA cleavage by MMP-7

The ability of the FA-QD-PA construct to function as a cleavable substrate was investigated as for the QD-PA precursor, described above.

2.7. Fluorescence measurements

Fluorescence measurements were obtained using a Nanodrop ND3300 fluorometer (Nanodrop Technologies, Wilmington, DE). Borate buffer (10 mM, pH 7.4) was used as the blank for both the absorbance and fluorescence. Fluorescence of all QDs was measured at 585 nm using an excitation at 470 ± 10 nm. Enzymatic cleavage of the QD-PA constructs was determined by measuring changes to the fluorescence spectra following incubation with MMP-7. The cleaved 5-FAM was separated from the QD construct using 100kD molecular weight cutoff filters. The spectra were scaled to normalize QD peak fluorescence (585nm) among all samples. The peak fluorescence intensity values at 520 nm and 585 nm were then directly compared to the spectra of control, uncleaved QD-PA particles to calculate the extent of PA construct cleavage following MMP-7 treatment.

2.8. Size measurements

Nanoparticle size was determined using dynamic light scattering (DLS) measurements conducted on a Malvern Nano Series Zetasizer with a 633 nm laser. The duration of each scan was 60 s and 3 scans were accumulated. The concentration of all QD samples for DLS assessment was 25 nM.

2.9. Statistics

One way analysis ANOVA tests were conducted using a $p \leq 0.001$ and a confidence interval of 95% (overall significance level of 0.05), unless otherwise noted. Student *t*-tests were conducted with a confidence interval of 99%.

3. Results and discussion

3.1. QD Functionalization and characterization

A dual ligand QD, functionalized with both the PA construct and the FA ligand was successfully synthesized and characterized. The PA construct was conjugated to the QD using an EDC coupling where the carboxylate group of the QD reacts with the N-terminus of the peptide. The c-terminus of the PA construct is capped with an amide to prevent further EDC conjugations, hence preventing aggregation [36]. By omitting NHS in the conjugation of PA to the QD, the EDC reaction is not as efficient and results in unreacted carboxylate groups [36]. These carboxylate groups are then available to react with another ligand. An EDC/NHS coupling reaction was used to functionalize the pre-synthesized QD-PA construct with folic acid (FA-QD-PA). The NHS

activates the carboxylic acid groups on the QDs, making them highly reactive toward amine nucleophiles [36]. The unreacted carboxylic acid groups react with the amine group on folic acid, resulting in the conjugation of a secondary ligand. For comparison purposes, a QD-PA and a QD-FA construct were synthesized using an EDC reaction.

Commercially available and chemically defined QDs were used in this study despite their well known potential for toxicity resulting from the CdSe constituents in the optical core. This work is focused on the development of fluorescence beacons that may be used as research materials in *in vitro* cell culture systems and animal models. The ease in sensing nanoconstruct characteristics and the reproducibility that is achieved through the use of commercially available materials is of considerable value, offsetting the limitations of dual-ligand nanoconstruct application due to QD core toxicity. The chemistries described in this work can be translated to the synthesis of dual-ligand nanoparticles with alternate core chemistries, including those with significantly reduced toxicity and potentially appropriate for use in humans. For example, nanoscale iron oxides functionalized as described in this work may be useful as *in vivo* reporters of biological activities for humans using magnetic resonance imaging as the detection tool.

For the FA-QD-PA nanoparticles, the addition of the PA construct was confirmed by dynamic light scattering (DLS), fluorescence measurements and gel electrophoresis. The nanoparticle construct experienced a statistically significant (one-way ANOVA) size increase upon the addition of the PA construct (Table 1). QD size increased from 18.2 ± 0.27 nm for unconjugated carboxylated QDs to 81.9 ± 10.5 nm for QDs functionalized with the PA construct. The statistically significant size increase indicates that the PA construct was successfully conjugated to the QD nanoparticle. Upon the addition of the FA to QD-PA, the size of the dual ligand construct (85.4 ± 2.3 nm) does not change significantly (one-way ANOVA), suggesting that FA ligand is shielded from interrogation by DLS and implying attachment to the QD, not to the end of the PA construct. Hydrophilic FA ligand conjugated to the end of the PA construct is likely to remain exposed at the PEG-water interface and available for DSL interrogation resulting in a detectable and significant additional size increase following conjugation.

Conjugation of the PA construct containing a 5-FAM label on the terminal end is confirmed by the emergence of a new fluorescence emission peak on the QD (Fig. 2A). The 5-FAM optical peak is distinct from the native QD fluorescence emission at 585. Gel electrophoresis was used to monitor the change in electrophoretic mobility mediated by the addition of the PA construct (Fig. 2B). The QD-PA construct (lane 7) had reduced electrophoretic mobility as compared to unmodified QDs (lane 5), consistent with successful PA conjugation. These results are in agreement with the analysis of Smith et al. [25]. The addition of folic acid was also confirmed using gel electrophoresis (Fig. 2B). The electrophoretic mobility of the FA-QD-PA construct (lane 8) was reduced as compared to the unmodified QDs (lane 5), QD-FA (lane 6) or the QD-PA construct (lane 7). Previously, Derfus et al. attached siRNA and a targeting peptide on a QD for siRNA delivery using reversible and non-reversible sulfide bonding [37]. In contrast to this work, we have functionalized two different ligands on a QD using a carefully titrated set of sequential covalent EDC reactions. By using the reactive amine and carboxylate functional groups that are common in synthetic peptides, proteins, and biomolecules for dual-ligand synthesis, we have developed a versatile, widely applicable technique for constructing second generation targeted nanoparticle therapies.

Table 1
Size of nanoparticle constructs.

Nanoparticle	Size (nm)	Standard deviation (nm)
Carboxylated QDs	18.2	0.3
QD-PA	81.9	10.5
FA-QD-PA	85.4	2.3

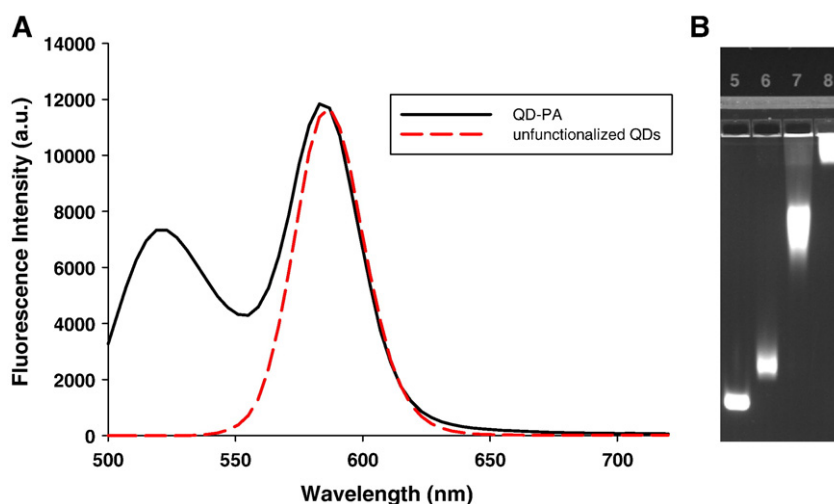


Fig. 2. A) Fluorescence spectra of unmodified QDs and the QD-PA conjugate. Addition of the PA construct, which includes a 5-FAM reporter with fluorescence emission at approximately 520 nm confirms the colocalization of the QD and PA construct. B) Gel electrophoresis of unmodified QDs (lane 5), QDs conjugated with folic acid (lane 6), QDs conjugated with PA (lane 7), and QDs conjugated with both PA and folic acid (lane 8). The relative electrophoretic mobilities of QD>QD-FA>QD-PA>FA-QD-PA are consistent with the expected nanomolecular structures.

3.2. FA-QD-PA cleavage by MMP-7

The ability of the FA-QD-PA construct to function as a cleavable substrate was investigated using exogenous MMP-7 [25]. While several studies have shown that MMP-7 is expressed by several tumor phenotypes, the exact concentration in the local area is unknown. Previously, *in vitro* studies have used concentration of up to 100 nM [25,38,39] while *in vivo* studies of other MMPs have documented similar concentrations [38, 39]. In this study, MMP-7 concentrations of 100 nM were used to test the FA-QD-PA construct.

Cleavage susceptibility of the FA-QD-PA construct was monitored using the physical separation of the QD from the 5-FAM molecule induced by MMP-7 activity. For comparison purposes, the enzymatic susceptibility of the nanoparticle QD-PA was also investigated. The intensity of the 520 nm peak of the FA-QD-PA conjugate following treatment with MMP-7 was compared to the intensity of the control sample (Fig. 3). 5-FAM fluorescence intensity of the FA-QD-PA construct decreased by $35.2 \pm 10.5\%$ after treatment with MMP-7. Loss of fluorescence intensity at 520 nm is consistent with MMP-7 mediated PA cleavage of the QD-PA construct measured here ($40.2 \pm 2.1\%$) as well as the unconjugated PA construct ($35.6 \pm 3.4\%$) [25]. Furthermore, PA

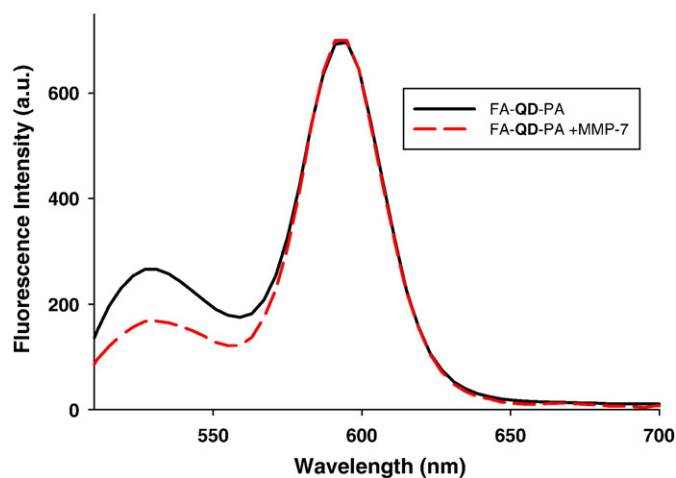


Fig. 3. The fluorescence spectra of FA-QD-PA conjugate exposed to MMP-7 and blank FA-QD-PA nanoparticles were compared. Approximately 30% of the PA construct was cleaved from the FA-QD-PA construct, a result statistically equal to the MMP-7 induced cleavage of 5-FAM from QD-PA and the unconjugated PA substrate in solution.

cleavage on the nanoparticles and for the unconjugated PA construct are not significantly different ($p < 0.001$, one-way ANOVA). PA cleavage from the QD that is also functionalized with folic acid is similar in extent to that measured for the QD-PA construct that lacks FA. These results suggest that the addition of the FA to the nanoparticle does not change the proteolytic susceptibility of the QD bound PA construct.

The molecular design of a dual-ligand nanoconstruct that can be translated to *in vivo* applications is a balance among multiple functional characteristics. We expect the nanoconstruct described here to be resistant to clearance by the reticuloendothelial system (RES) *in vivo*. The overall molecular mass of the PA component (primarily controlled by the molecular masses of the proximal and distal PEG) is likely to have significant influence on the cardiovascular persistence of the nanoconstruct. The overall PA length in this work has been selected based on PEGylated nanoparticles with extended cardiovascular half-life described in literature and through preliminary syntheses (results not shown). The distal PEG size on the PA component will presumably modulate the rate of PA cleavage through partial control of enzyme access to the peptide. Transport of the enzyme from the bulk fluid phase to the peptide occurs through the distal PEG and is likely to be influenced by distal PEG molecular mass. The relative lengths of the PEGs on the PA constituent will control the presentation of the folic acid following PA cleavage and the potential for folic acid access in the uncleaved state. Ideally, the folic acid should be concealed prior to cleavage and accessible following cleavage, since cellular recognition of the nanoconstruct depends on folic acid accessibility. These are conflicting requirements that require an optimized balance among the molecular masses of the PEGs. PEG molecular masses used in the current implementation have been selected based on first principles of molecular and nanoscale structure/function understanding. Additional studies to assess the roles of proximal and distal PEG molecular masses on nanoconstruct performance are likely to result in additional activity optimization.

4. Conclusion

PA targeting requires the colocalization of the cleavable masking agent and the concealable ligand. In this work, a PA targeted QD has been successfully designed, synthesized and characterized. Using sequential EDC reactions, the PA construct and folic acid were covalently attached to the QD. The addition of folic acid to the QD-PA does not affect the substrate susceptibility to MMP-7. Subsequent work will explore the ability of the NP probe described here to assess

PA targeting *ex vivo* and *in vivo* by quantitative fluorescence measurements and fluorescence imaging. This laboratory has demonstrated the capacity for single-ligand nanoconstructs with similar PA chemistry to be exhaustively cleaved at enzyme concentrations of 100 nM and with significant cleavage in the presence of as little as 5 nM of MMP-7 enzyme [25]. MMP-7 concentrations *in vivo* have been reported to be at least 100 nM [38,39], suggesting that the current nanoconstruct can be cleaved *in vivo*. Achieving significant MMP-7 secretion from cultured cells, however, is a challenge. In addition, cell culture media plays a profound role in modulating the capacity for MMP-7 synthesis. While the use of QDs in clinical applications is unlikely due to their potential for unintended cytotoxicity, the strategy for PA targeting described herein could be applied to other nanoparticle cores. Nanoparticle cores with particular practical potential include iron oxides for MR imaging, gold nanoparticles for PET imaging and dendrimers or liposomes for targeted drug delivery.

Acknowledgement

The authors gratefully acknowledge the Department of Defense, Congressionally Directed Medical Research Program, Breast Cancer Research Program Idea Award BC043908 for funding.

References

- [1] M.S. Sachdeva, Expert Opin. Investig. Drugs 7 (1998) 1849.
- [2] D.E. Hallahan, L. Geng, A.J. Cmelak, A.B. Charkravathy, W. Martin, C. Scarfone, A. Gonzalez, J. Control. Release 74 (2001) 183.
- [3] F. Pastorino, C. Brignole, D. Marimpietri, M. Cilli, C. Gambini, D. Ribatti, R. Longhi, T.M. Allen, A. Corti, M. Ponzoni, Cancer Res. 63 (2003) 7400.
- [4] A. Mitra, J. Mulholland, A. Nan, E. McNeill, H. Ghandehari, J. Control. Release 102 (2005) 191.
- [5] T. Bogenrieder, M. Herlyn, Oncogene 22 (2003) 6524.
- [6] R. Kim, T. Toge, Surg. Today 34 (2004) 293.
- [7] R. Weissleder, C.-H. Tung, U. Mahmood, A. Bogdanov, Nat. Biotechnol. 17 (1999) 375.
- [8] C.-H. Tung, U. Mahmood, S. Bredow, R. Weissleder, Cancer Res. 60 (2000).
- [9] J.O. McIntyre, L.M. Matrisian, J. Cell. Biochem. 90 (2003) 1087.
- [10] T.D. Harris, G. von Maltzahn, A.M. Derfus, E. Ruoslahti, S. Bhatia, Angew. Chem., Int. Ed. 45 (2006) 3161.
- [11] H. Yao, Y. Zhang, F. Xiao, Z. Xia, J. Rao, Angew. Chem., Int. Ed. 46 (2007) 4346.
- [12] J.O. McIntyre, B. Fingleton, S.K. Wells, D.W. Piston, C.C. Lynch, S. Gautam, L.M. Matrisian, Biochem. J. 377 (2004) 617.
- [13] T. Suzawa, S. Nagamura, H. Saito, S. Ohta, N. Hanai, J. Kanazawa, M. Okabe, M. Yamasaki, J. Control. Release 79 (2002) 229.
- [14] T. Suzawa, S. Nagamura, H. Salto, S. Ohta, N. Hanai, M. Yamasaki, J. Control. Release 69 (2000) 27.
- [15] C. Lui, C. Sun, H. Huang, K. Janda, T. Edgington, Cancer Res. 63 (2003) 2957.
- [16] P. Basset, O.A. M.P. Chenard, R. Kannan, I. Stoll, P. Anglard, J.P. Bellop, M.C. Rio, Matrix Bio. 15 (1997) 535.
- [17] M. Johnsen, L.R. Lund, J. Romer, K. Almholt, K. Dano, Curr. Opin. Cell Biol. 10 (1998).
- [18] B.E. Bachmeier, A.G. Nerlich, R. Lichtinghagen, C.P. Sommerhoff, Anticancer Res. 21 (2001) 3821.
- [19] H. Tanimoto, L.J. Underwood, K. Shigemasa, T.H. Parmley, Y. Wang, Y. Yan, J. Clarke, T.J. O'Brien, Tumor Biol. 20 (1999) 88.
- [20] P. Vihinen, V.-M. Kahari, Int. J. Cancer 99 (2002) 157.
- [21] H. Yamamoto, Y. Adachi, F. Itoh, S. Iku, K. Matsuno, M. Kusano, Y. Arimura, T. Endo, Y. Hinoda, M. Hosokawa, K. Nasaolmai, Cancer Res. 59 (1999) 3313.
- [22] H. Yamamoto, F. Itoh, S. Iku, Y. Adachi, H. Fukushima, S. Sasaki, M. Mukaiya, K. Hirata, K. Imai, J. Clin. Oncol. 19 (2001) 1118.
- [23] H.C. Crawford, C.R. Scoggins, M.K. Washington, L.M. Matrisian, S.D. Leach, J. Clin. Invest. 109 (2002) 1437.
- [24] D.L. Hulboy, S. Gautam, B. Fingleton, L.M. Matrisian, Oncol. Rep. 12 (2004) 13.
- [25] R.A. Smith, S.L. Sewell, T.D. Giorgio, J. of Inter. Nanomed. 3 (2008) 95–103.
- [26] B. Ballou, B.C. Langerholm, L.A. Ernst, M.P. Bruchez, A.S. Waggoner, Bioconjug. Chem. 16 (2004) 1488.
- [27] E.L. Bentzen, I.D. Tomlinson, J. Mason, P. Gresch, M.R. Warnement, D. Wright, E. Sanders-Bush, R. Blakely, S.J. Rosenthal, Bioconjug. Chem. 16 (2005) 1488.
- [28] D. Pan, J.L. Turner, K.L. Wooley, Chem. Commun. (2003) 2400.
- [29] J.F. Kukowska-Latallo, K.A. Candido, Z. Cao, S.S. Nigaveka, I.J. Majoros, T.P. Thomas, L.P. Balogh, M.K. Khan, J. Baker, R. James, Cancer Res. 65 (2005) 5317.
- [30] N. Parker, M.J. Turk, E. Westrick, J.D. Lewis, P.S. Low, C.P. Leamon, Anal. Biochem. 338 (2005) 284.
- [31] L.C. Hartmann, G.L. Keeney, W.L. Lingle, T.J.H. Christianson, B. Varghese, D. Hillman, Int. J. Cancer 121 (2007) 938.
- [32] S.D. Weitman, R.H. Lark, L.R. Coney, D.W. Fort, V. Frasca, V.R. Zurawski, B.A. Kamen, Cancer Res. 52 (1992) 3396.
- [33] J. Holm, S.I. Hansen, M. Hoier-Madsen, L. Bostad, Biochem. J. 280 (1991) 267.
- [34] M.D. Kennedy, K.N. Jallad, J. Lu, P.S. Low, D. Ben-Amotz, Pharm. Res. 20 (2003) 714.
- [35] T.A. Patrick, D.M. Kranz, T.A. van Dyke, E.J. Roy, J. Neuro-Oncol. 32 (1997) 111.
- [36] G.T. Hermanson, Bioconjugate Techniques, Academic Press, San Diego, 1996.
- [37] A.M.C. Derfus, Alice A., Dal-Hee Min, Erkki Ruoslahti, Sangeeta N. Bhatia, Bioconjug. Chem. 18 (2007) 1391.
- [38] M. Kioi, K. Yamamoto, S. Higashi, N. Koshikawa, K. Fujita, K. Miyazaki, Oncogene 22 (2003) 8662.
- [39] F.-Q. Wang, J. So, S. Reierstad, D.A. Fishman, Int. J. Cancer 114 (2005) 19.